water

MDPI

Article

Impacts of Urbanization on Variations of Extreme Precipitation over the Yangtze River Delta

Congxuan Kang [1,2], Zujiang Luo [1,*], Wen Zong [3] and Jian Hua [2]

1 School of Earth Sciences and Engineering, Hohai University, Nanjing 210098, China; CongxKang_cgs@163.com
2 Engineering Innovation Center for Urban Underground Space Exploration and Evaluation, Ministry of Natural Resources of the People's Republic of China, Nanjing 210014, China; JianHua_cgs@163.com
3 Geological Survey and Research Institute of Jiangsu Province, Nanjing 210014, China; sharkshark00@sina.com
* Correspondence: ZujLuo_HHU@163.com

Abstract: The urbanization process is the hallmark of the population's economic activities and land-use types, including population-, economic-, and landscape-urbanization. The question of how to classify the stations into urbanized and suburbanized stations is important for detecting the contribution rates of urbanization to precipitation extremes. This study used the fuzzy c-means clustering method to classify different urbanized level stations by population, economy, and impervious surface in the Suzhou-Wuxi-Changzhou urban agglomeration. Based on the change trends of six extreme precipitation indices, the contribution rates of urbanization to the precipitation extremes were estimated. The results show that the increasing indices were the intensity indices, while the decreasing indices were the duration indices during 1980–2015. Moreover, high urbanization tended to have a higher contribution to the most extreme precipitation indices, especially the intensity indices, than urbanization in the medium-size cities, indicating the urbanization leads to the phenomenon of extreme precipitation enhancement. The results of the three kinds of classification methods were different, especially the classification by the impervious area. This paper investigated the spatiotemporal changes in precipitation extremes and the contribution of urbanization to extreme precipitation, which will provide support for the development of urban agglomeration in the future.

Keywords: contribution rate; extreme precipitation; urbanization impacts; clustering method; Yangtze River Delta

check for updates

Citation: Kang, C.; Luo, Z.; Zong, W.; Hua, J. Impacts of Urbanization on Variations of Extreme Precipitation over the Yangtze River Delta. *Water* **2021**, *13*, 150. https://doi.org/10.3390/w13020150

Received: 10 December 2020
Accepted: 7 January 2021
Published: 10 January 2021

1. Introduction

Extreme rainfall events are one of the most frequent natural disasters around the world, which brings huge economic losses to human society. The changing of extreme rainfall is not only caused by the internal forces of the climatic system (e.g., solar radiation), but also by human activities (e.g., changes of land cover types and emission of greenhouse gases) [1,2]. With the increasing population and the expanding impervious surfaces, the urbanization process is an important human activity [3,4]. The dense population in urban agglomerations is sensitive and vulnerable to climatic disasters. Therefore, it is essential to detect the impact of urbanization on the variations of extreme rainfall in flood risk management.

Many studies showed that the urbanization process had a significant influence on the formation and changes of extreme precipitation [5–7]. Horton (1921) firstly found that the frequency of heavy rain in urban areas was higher than that in suburbs through observed data in multiple cities [8]. Subsequently, the Metropolitan Meteorological Experiment (METROMEX) was carried out in the United States and found that the rainfall intensified significantly in the city center and its downwind regions [9,10]. With the development of meteorological radar and satellite, obtained remote sensing data has provided observed data with higher spatial and temporal resolution. Shepherd and Burian (2003) found that the summer rainfall increased by 28% in the range of 30–60 km downwind regions from the city based on satellite rainfall data [11]. At the same time, the improvement of computer technology has provided a numerical simulation technology (e.g., the weather research and forecasting model, WRF) to detect quantitatively the physical mechanisms of urbanization on rainfall in New York [12], Europe [13], Singapore [14], and China [15,16]. These studies have concluded that the development of urbanization has had a certain impact on rainfall, but the contribution rates of urbanization on the extreme precipitation is still an open question.

Regarding the contribution of urbanization on extreme rainfall, physical modeling and statistical analysis are popular methods currently [17–20]. For example, Yang et al. (2019) explored the temporal and spatial distribution of rainfall based on the WRF model in large urbanized regions [21]. Unfortunately, the physical modeling process has some limitations, such as the existing uncertainties of the model parameters, the requirement of high-resolution data, and the relatively large computational cost. Conversely, the statistical analysis using observed data requires a simple computing process and applies to a smaller region [22]. Previous studies compared the variations of the rainfall characteristics (e.g., the intensity and duration of rainfall events) between different urbanized development stages in the same stations [23,24], and between different stations during the same period [25–28]. In these studies, the classification of the stations into urban and rural stations usually based on the administrative attributes. However, the classification of the stations into urban and rural stations has a determining influence on the study results. The urbanization process is the hallmark of population economic activities and land-use types, including population urbanization, economic urbanization, and landscape urbanization [29,30]. This study will classify the observed stations according to the different urbanization (i.e., population urbanization, economic urbanization, and landscape urbanization) by objective clustering criteria, which is the novelty of this study.

Suzhou-Wuxi-Changzhou urban agglomeration (abbreviated as SXC) has become one of the regions with the fastest and highest urbanized development in eastern China. The overall aim of this work is to estimate the contribution rates of urbanization on the extreme precipitation based on different classification results of the stations. The sections of this study are three-fold: we (1) classify the rainfall stations into highly urbanized stations, town stations, and rural stations by population, economy, and impervious surface through a clustering method, (2) detect the variation trend of the extreme precipitation indices from 1980 to 2015, and (3) estimate the contribution rates of urbanization on the extreme precipitation. Our results will provide a reference for flood prevention and disaster reduction in this area.

2. Materials and Methods

2.1. Study Region

The Suzhou-Wuxi-Changzhou urban agglomeration (32.17° N–30.71° N, 119.27° E–121.05° E) is located in the core region of the Yangtze River delta and covers an area of 17,199 km^2 (Figure 1), including Suzhou, Wuxi, and Changzhou in Jiangsu province. As one of the largest urban agglomeration in eastern China, the SXC region has a massive population and developed economy during the past decades. Taking Suzhou as an example, the resident population increases from 5610.2 thousand in 1990 to 6500.1 thousand in 2015. The gross domestic product increases from RMB 20,214 million yuan in 1990 to RMB 1,450,407 million yuan in 2015. The rapid urbanization process has brought dramatic changes in the land cover, resulting in floods or other water disasters [31,32]. The SXC region is a typical region for detecting the influences of the urbanization process on extreme precipitation.

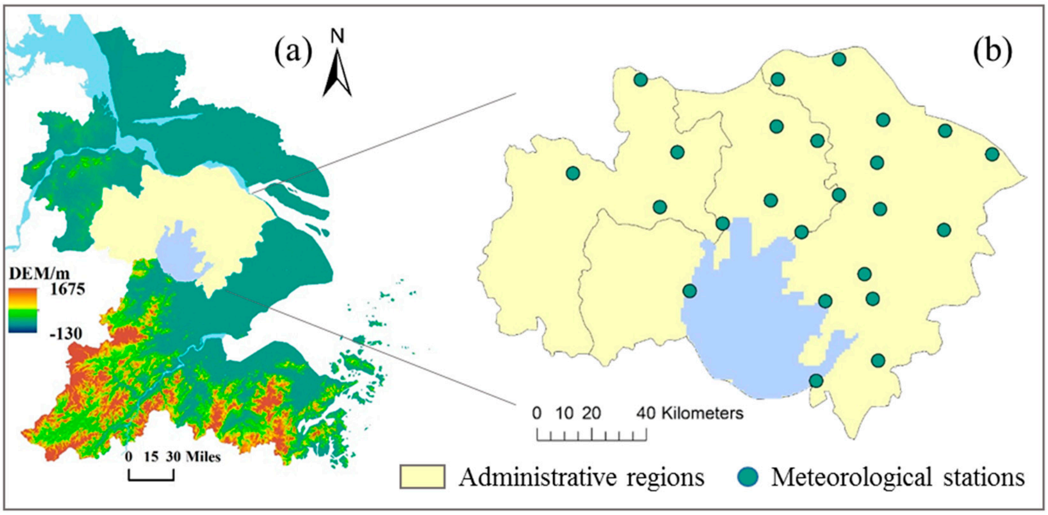

Figure 1. The location of the study region (**a**) and spatial distribution of meteorological stations (**b**).

2.2. Datasets

After being quality-controlled, daily precipitation data were obtained from Taihu Hydrological Yearbooks during 1980–2015. The distribution of meteorological stations is shown in Figure 1. Considering the local climate in the SXC urban agglomeration, six extreme precipitation indices (Table 1) were calculated from daily precipitation data during 1980–2015 [33,34]. Specifically, CDD and CWD denote the duration indices; PRCPTOT denotes the total precipitation, and other indices denote the precipitation intensity.

Table 1. Definitions of extreme precipitation indices.

Index	Description	Definition	Unit
CDD	Consecutive Dry Days	Maximum number of consecutive days (daily precipitation < 1 mm)	d
CWD	Consecutive Wet Days	Maximum number of consecutive days (daily precipitation $\geq$ 1 mm)	d
SDII	Simple Daily Intensity Index	Annual precipitation divided by the number of wet days	mm/d
Rx1day	Maximum One-Day Precipitation	Maximum daily precipitation amount	mm
Rx5day	Maximum Five-Day Precipitation	Maximum five-day precipitation amount	mm
PRCPTOT	Total Wet-Day Precipitation	Annual precipitation amount	mm

The population dataset (POP) and gross domestic product (GDP) dataset for 2015 were downloaded on the website of the Chinese Resource and Environment Data Cloud Platform, with a spatial resolution of 1 km. The impervious surface map for 2015 was obtained from the global artificial impervious area (IAP) Dataset with a spatial resolution of 30 m [35] (http://data.ess.tsinghua.edu.cn). Moreover, the IAP dataset was resampled as a spatial resolution of 1 km, which accords with POP and GDP datasets.

2.3. Methods

The flowchart of our methods is shown in Figure 2.

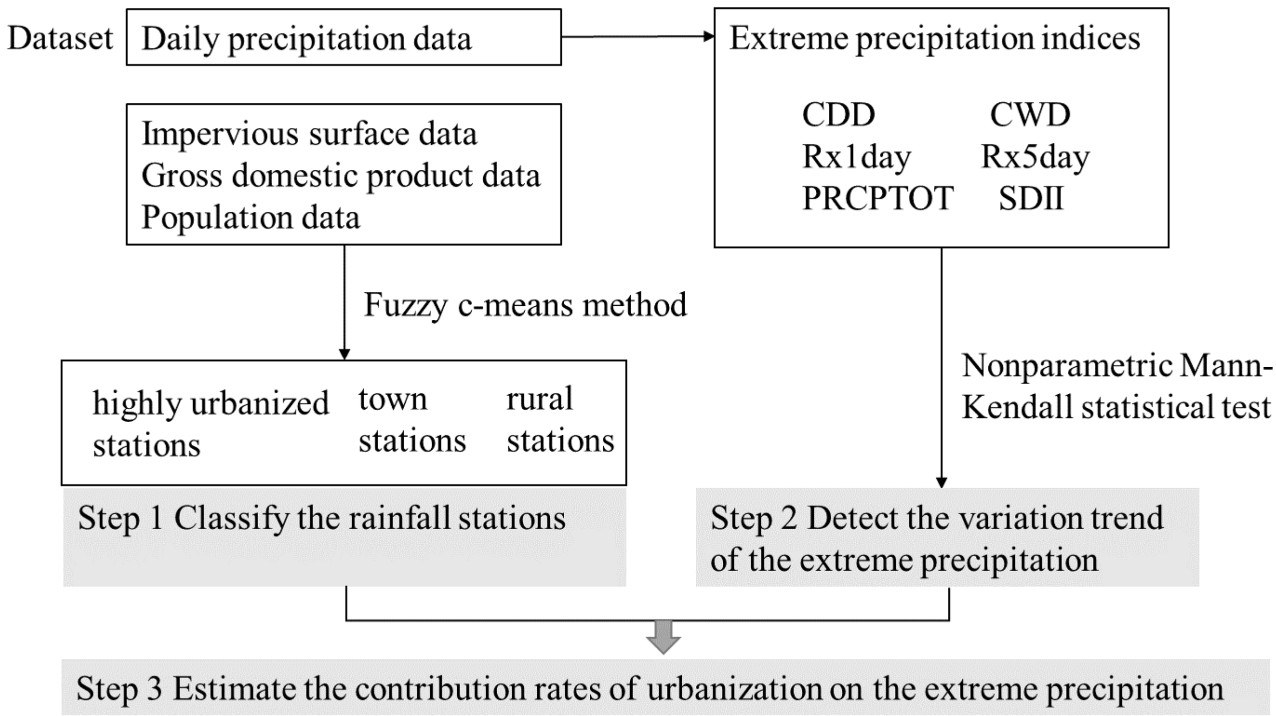

Figure 2. The flowchart of our methods.

2.3.1. Clustering Method for Classification

Selecting an optimal clustering method for classifying meteorological stations is important to get reliable results for our study aims. The fuzzy c-means (FCM) is a kind of fuzzy clustering algorithms with an unsupervised learning classification algorithm. The FCM algorithm has a simple process and a fine partition it usually produces [36,37]. Thus, this study used the fuzzy c-means clustering method to classify different urbanized level stations by population, economy, and impervious surface in the Suzhou-Wuxi-Changzhou urban agglomeration.

Assuming $\{a_{ij}\}$ are the values of a matrix A, the membership matrix of the dataset can be initialized as [37]:

$$\sum_{I=1}^{C} a_{ij} = 1, \ \ \forall j = 1, \ldots, n \tag{1}$$

where a_{ij} is a membership value, i is the row number and j is the column number.

The dissimilarity function in the FCM algorithm can be defined as:

$$\mathrm{J}(\mathrm{A}, \ c_1, c_2, \ldots, c_c) = \sum_{i=1}^{c} \sum_{j=1}^{n} a_{ij}^{m} D_{ij}^{2} \tag{2}$$

where c_i is the cluster centroid; D_{ij} is the Euclidian distance between the ith centroid and jth data point; n is the number of the clusters, and m is a weighting exponent which takes a value between 1 and ∞.

To minimize the dissimilarity functions by simulating the center vectors, an iterative optimization algorithm is defined as:

$$c_i = \sum_{j=1}^{n} a_{ij}^{m} x_i / \sum_{j=1}^{n} a_{ij}^{m} \tag{3}$$

$$a_{ij} = \frac{1}{\sum_{k=1}^{c} \left(\frac{D_{ij}}{D_{kj}}\right)^{\frac{2}{m-1}}} \tag{4}$$

where x_i is the ith data point, and k is the iteration step. θ is a termination criterion that has been defined. The interaction will stop when $\{\,||a_{ij}{}^{k+1} - a_{ij}{}^{k}||\,\} \leq \theta$.

2.3.2. Trend Changes

The nonparametric Mann-Kendall statistical test (MK test) is a popular trend test in extreme precipitation [38].

In the MK test, for a dataset X = $x_1, x_2, \ldots, x_n$, the statistic S is calculated by [39]:

$$S = \sum_{i=1}^{n-1} \sum_{j=i+1}^{n} sgn\left(x_j - x_i\right) \tag{5}$$

$$sgn\left(x_j - x_i\right) = \begin{cases} 1 & x_j > x_i \\ 0 & x_j = x_i \\ -1 & x_j < x_i \end{cases} \tag{6}$$

where n is the dataset length, $x_{i(j)}$ is the ranked value of the dataset.

The variance of an independent and identically distributed series with zero mean is defined as:

$$var(S) = n(n-1)(2n+5)/18 \tag{7}$$

The Z value of the MK test can be estimated by:

$$Z = \begin{cases} \frac{S-1}{\sqrt{var(S)}}, & S > 0 \\ 0, & S = 0 \\ \frac{S+1}{\sqrt{var(S)}}, & S < 0 \end{cases} \tag{8}$$

A positive value shows an increasing trend, while a negative value shows a decreasing trend.

The Sen's slope β denotes the changing degree of the trend, which is estimated as:

$$\beta = \text{Median}\left[\left(x_j - x_i\right)/(j-i)\right] \tag{9}$$

where $1 < i < j < n$, β is Sen's slope.

2.3.3. Contribution of Urbanization to Precipitation Extremes

The weather stations were classified into three classifications: level 1, level 2, and level 3 through the fuzzy clustering algorithm. Specifically, level 1 indicates the stations distributed in rural regions; level 2 denotes the stations distributed in suburban regions, and level 3 represents the stations distributed in highly urbanized regions.

The contribution rates of urbanization to extreme precipitation are the percent proportion of urbanization on the trends of precipitation extremes. The trends of extreme precipitation indices in the three levels of stations are estimated by Sen's slope. $\triangle j_1$ denotes the contribution rate of urbanization to extreme precipitation, and its equations are as follows [40].

$$\triangle j_1 = \left|\frac{\beta_j - \beta_1}{\beta_j}\right| \times 100\%, \quad j = 2,\ 3 \tag{10}$$

where β_j (j = 2, 3) denotes the slopes of the trends of extreme precipitation indices for stations in level 2 and level 3 stations; β_1 denotes the slope of the trends for stations in level 1. If $\triangle j_1 > 0$, urbanization increases the extreme precipitation indices; if $\triangle j_1 < 0$, urbanization decreases the extreme precipitation indices; if $\triangle j_1 = 0$, urbanization has no effects on the extreme precipitation indices; and if $\triangle j_1 = 100\%$, the trend of the extreme precipitation indices is completely caused by urbanization. Especially, in the calculation process, $\triangle j_1 > 100\%$ indicates that urbanization has a strong impact on the trend of extreme precipitation, and the extra trend might be caused by other unidentified factors. In this case, $\triangle j_1$ should be set to 100%.

3. Results and Discussion

3.1. Classification of Stations in Different Urbanized Levels

The stations were clustered into three urbanization levels in accordance with economic urbanization, population urbanization, and land urbanization, respectively. The lowly urbanized stations have relatively low population density, low GDP, and high permeable surface area. Conversely, the highly urbanized stations have dense population density, high GDP, and high impervious surface area. The characteristics of the medially urbanized stations are in between. Specifically, level 1 indicates the stations distributed in rural regions; level 2 denotes the stations distributed in suburban regions, and level 3 means the stations distributed in highly urbanized regions. Figure 3a–c depicts the spatial distributions of GDP, POP, and IAP.

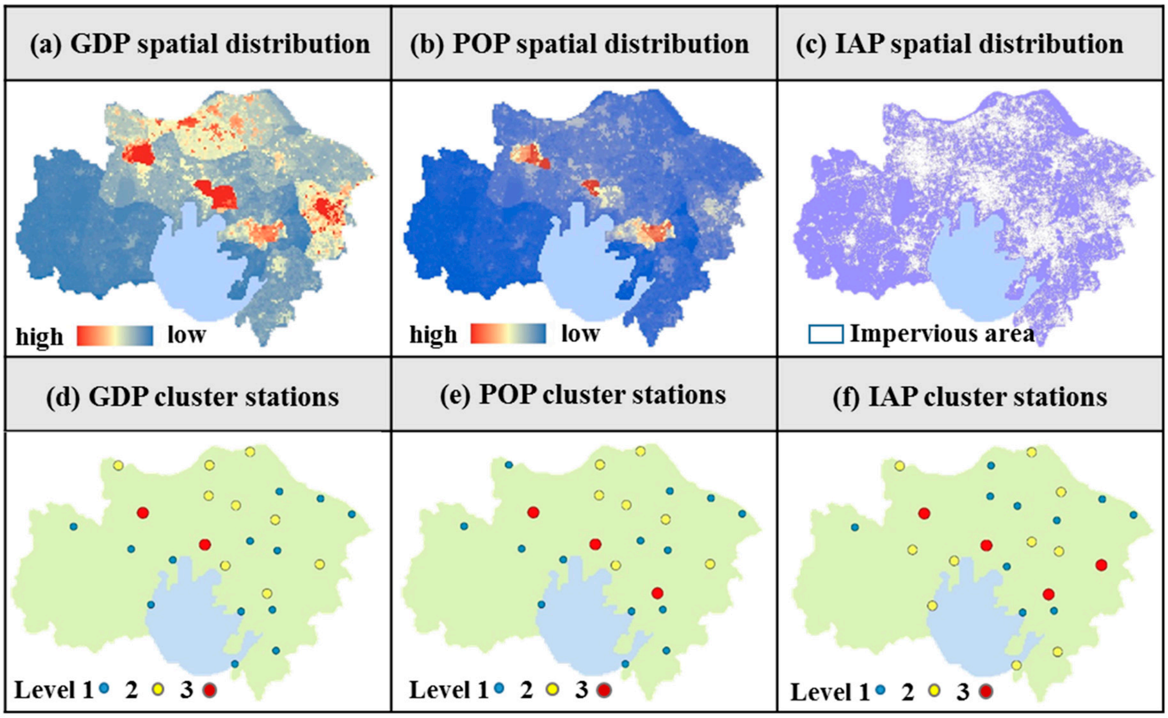

Figure 3. The spatial distributions of gross domestic product (GDP) (**a**), population dataset (POP) (**b**), and global artificial impervious area (IAP) (**c**); results of the classification stations: GDP (**d**), POP (**e**), and IAP (**f**).

Figure 3d–f shows the results of the classification stations. The observed stations in each urbanized level have the same local climate characteristics, which are well distributed over the region. The results of classification by population are similar to those of classification by GDP. Stations in Level 3 are within Changzhou, Suzhou, Wuxi, and Kunshan for the three cluster references. Cities such as Changzhou, Suzhou, and Wuxi are large cities in the Yangtze River Delta and contributed a massive population and economy to the urbanization process. Meanwhile, Changshu and Kunshan experienced relatively low urbanization growth with relatively lower GDP and higher IAP. Stations in Level 2 have the largest amount and are located in the surrounding regions of the level 3 stations. Moreover, the stations in level 1 clustered by impervious surfaces have a smaller number of stations than that by economy and population. This is because the impervious surfaces of Changzhou, Suzhou, and Wuxi have been expanding recently, whereas the GDP and population are relatively low in the boundary of the impervious surface.

3.2. Spatiotemporal Changes of Precipitation Extremes

The spatial patterns of six extreme precipitation indices were interpolated by the inverse distance weighting method. As shown in Figure 4, CDD has a similar distribution with SDII, which has the lowest values in Changzhou city. The spatial pattern of Rx1day is similar to that of Rx5day and CWD, which has high values in the western Changzhou region and low values in the southern Suzhou region. Otherwise, the spatial distribution of PRCPTOT is contrary to Rx1day and Rx5day. Moreover, it was found that the intensity of extreme precipitation is high in the western Changzhou region and low in the southern Suzhou region. The total amount of extreme precipitation has a contrary distribution to the intensity of extreme precipitation.

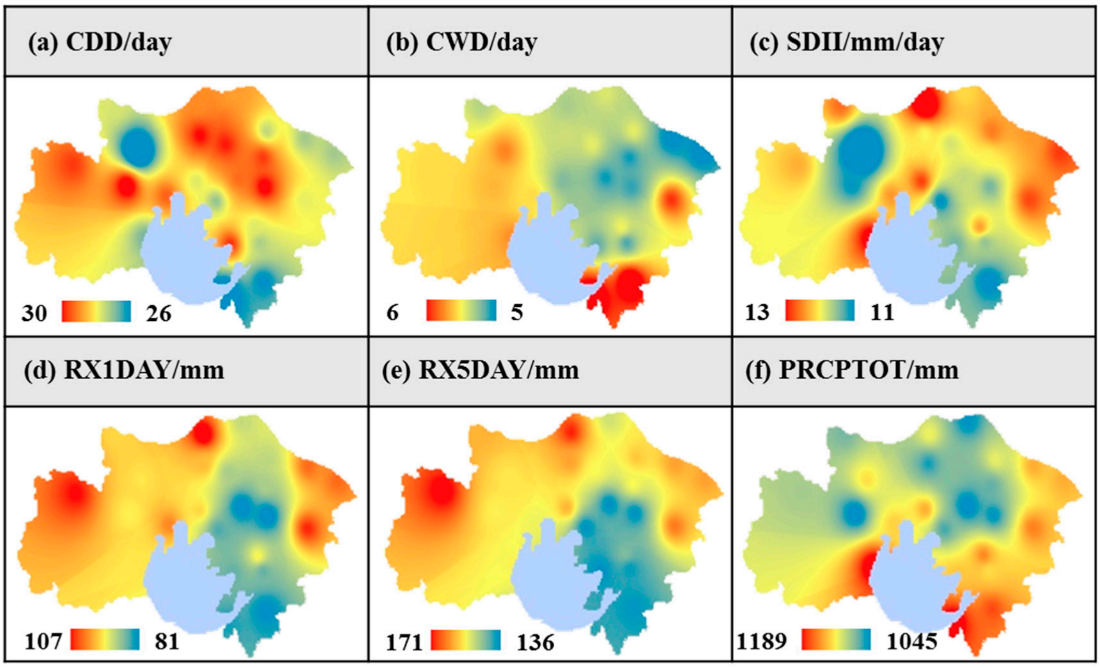

Figure 4. The spatial patterns of six extreme precipitation indices for the three urbanization levels during 1980–2015: CDD (**a**), CWD (**b**), SDII (**c**), RX1DAY (**d**), RX5DAY (**e**), and PRCPTOT (**f**).

Figure 5 describes the temporal trends of the precipitation extremes for the stations in three urbanized levels during 1980–2015. CDD and CWD indices had decreasing trends, and the others had increasing trends. Furthermore, the decreasing indices were both the duration indices, while the increasing indices were the intensity indices. The largest increasing trend was observed for Rx1day by population classified reference and the largest decreasing trend was seen for CDD by impervious surface classified reference. The trends for CDD, CWD, and Rx1day for GDP classified reference, CWD for population classified reference were all statistically significant in level 3. The change trends of Rx1day are significantly increasing in the three types of stations.

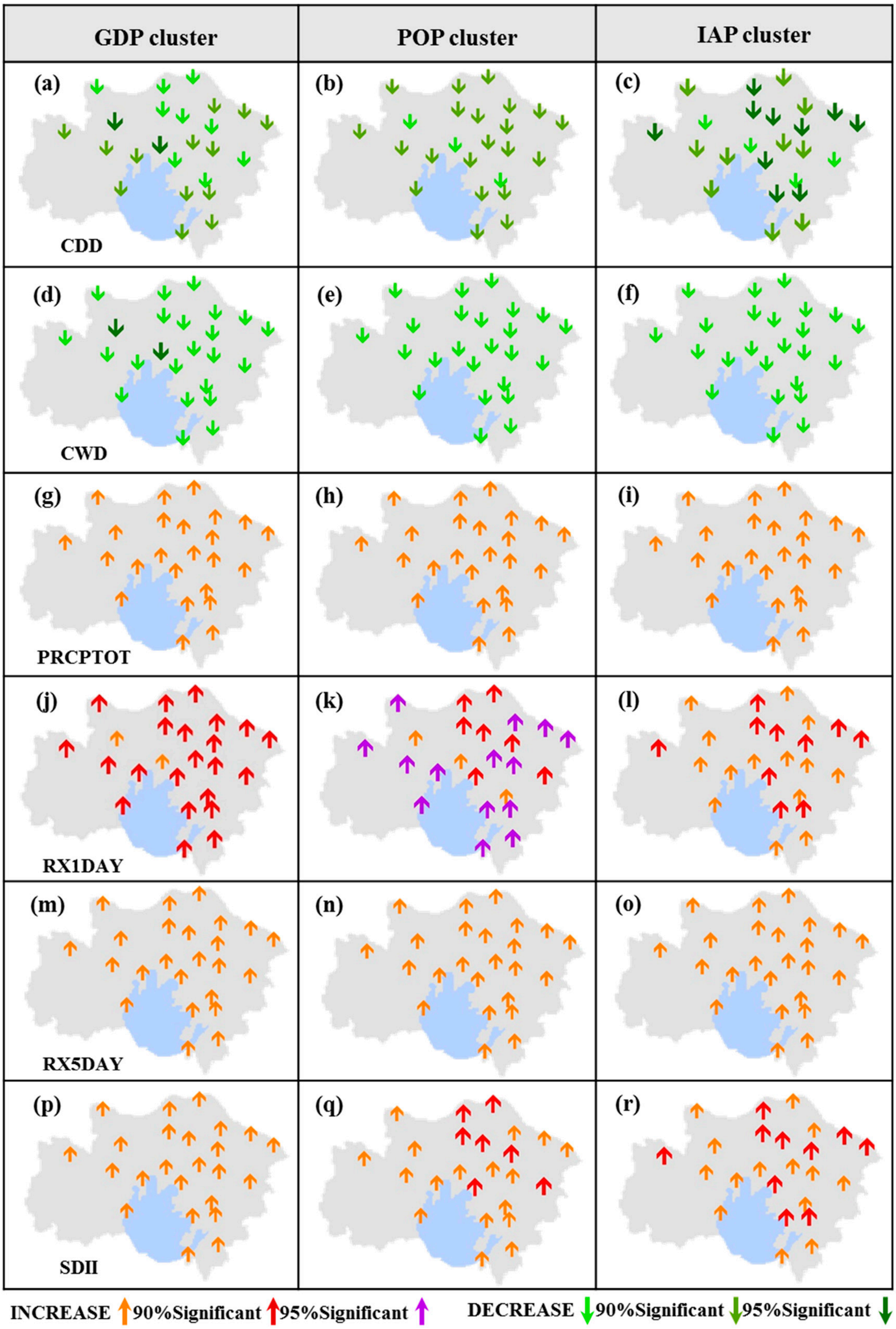

Figure 5. The temporal trends of precipitation extremes for the stations in three urbanized levels during 1980–2015. The results of GDP cluster: CDD (**a**), CWD (**d**), PRCPTOT (**g**), RX1DAY (**j**), RX5DAY (**m**), and SDII (**p**). The results of POP cluster: CDD (**b**), CWD (**e**), PRCPTOT (**h**), RX1DAY (**k**), RX5DAY (**n**), and SDII (**q**). The results of IAP cluster: CDD (**c**), CWD (**f**), PRCPTOT (**i**), RX1DAY (**l**), RX5DAY (**o**), and SDII (**r**).

3.3. Contribution Rates of Urbanization on Precipitation Extremes

The contribution rates of urbanization to extreme precipitation in three-level stations by different classification references are shown in Table 2. For the results of classification by population, urbanization has significant impacts on CDD, Rx1day, and Rx5day in level 3 stations, and have more impacts on extreme precipitation in level 1 stations than that in level 2 stations, except SDII. Specifically, urbanization has a high influence on SDII in level 2 stations, reach to 84.79%. Urbanization has a low influence on CDD and PRCPTOT in level 2 stations, reach to 12.25% and 9.14%, respectively. Urbanization has little influence on Rx1day in level 2 stations, just 0.85%. The results of classification by GDP are similar to those of classification by population. However, the results of classification by impervious surfaces are different from those of classification by population and GDP. Urbanization has significant impacts on CDD and Rx5day in level 3 stations and no significant impacts on CWD and SDII. Urbanization has significant impacts on PRCPTOT, Rx1day, and SDII in level 2 stations.

Table 2. The effects of urbanization on extreme precipitation in three-level stations by different classification references.

Unit/%	CDDΔ2-1	CDDΔ3-1	CWDΔ2-1	CWDΔ3-1	PRCPTOTΔ2-1	PRCPTOTΔ3-1	RX1Δ2-1	RX1Δ3-1	RX5Δ2-1	RX5Δ3-1	SDIIΔ2-1	SDIIΔ3-1
POP	12.3	100	75.9	84.2	9.1	58.1	0.8	100	48.7	100	84.8	35.7
GDP	64.9	41.4	38.3	81.6	25.1	32.4	0.8	100	4.45	26.3	82.8	38.3
IAP	82.4	100	28.5	0	100	42.1	100	88.5	42.6	100	100	0

By comparing the contribution rates of urbanization on extreme precipitation by three kinds of classifications, we found that the contribution rates of urbanization to extreme precipitation in level 3 stations are higher than those in level 2 stations except CDD and SDII, which means the contribution rates of most extreme precipitation indices are higher in the city than that in the rural region, indicating the urbanization lead to the phenomenon of extreme precipitation enhancement. The results of the three kinds of classification methods are different, especially the classification by the impervious area. This is because the rural regions usually have many impervious surfaces due to urbanization while these regions have low population density and economic development. It may be revealed that the classification by impervious surface is not suitable for this study.

3.4. Discussion

Our results found that high urbanization tended to have a higher contribution to most extreme precipitation indices, especially the intensity indices, than urbanization in the medium-size cities, indicating the urbanization lead to the phenomenon of extreme precipitation enhancement. To validate our results, we figured out the frequency of the year when the top 50 maximum daily rainfalls occurred during 1980–2016 in the four typical stations (i.e., Changzhou, Baishaoshan, Wuxi, and Ganlu). Changzhou and Wuxi stations denote the highly-urbanized stations, while Baishaoshan and Ganlu stations denote the lowly-urbanized stations. From Figure 6 it can be seen that the occurrence of the high intensity is higher in the highly-urbanized stations than in the lowly-urbanized stations from 1980 to 2016, which can validate our results. Thus, using the differences of observations to reflect the contribution of urbanization on extreme precipitation is relatively reliable and realistic.

Moreover, our method is feasible to the region with dense stations, not applicable to the region with sparse stations. The spatial and temporal changes in local precipitation are affected by a variety of factors, such as the urban heat island effect, canopy barrier effect, and aerosol emissions. Meanwhile, the local climate is not the determining factor in the formation of extreme precipitation under the global climate background. Therefore, a more comprehensive investigation on the influence mechanism of urbanization on extreme precipitation from a global perspective is needed in further research.

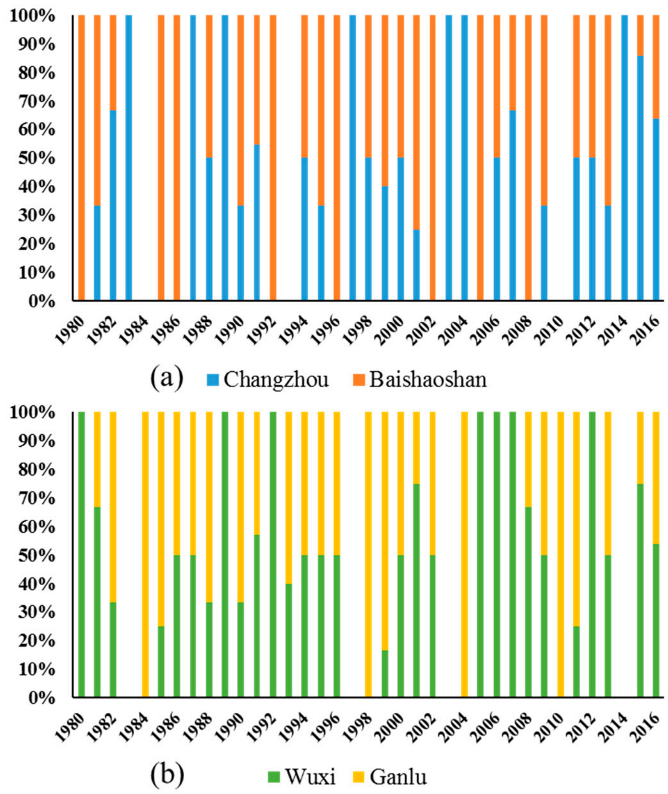

Figure 6. The occurrence of the high intensity in the highly-urbanized stations and the lowly-urbanized stations from 1980 to 2016. The results of (**a**) Changzhou station and Baishaoshan station and (**b**) Wuxi station and Ganlu station.

4. Conclusions

To detect the contribution rates of urbanization to precipitation extremes, this paper used the difference between stations with different urbanized levels in the SXC region. We found some conclusions as follows.

(1) It is feasible to classify the stations in different urbanized levels determined by population, economy, and land type via the fuzzy c-means clustering method. However, the classification by impervious surface is not suitable for this study.

(2) During 1980–2015, different extreme rainfall indices have different trends in our region. The intensity indices (e.g., PRCPTOT, SDII, Rx1day, and Rx5day) showed increasing trends, while the duration indices (e.g., CDD and CWD) showed a decreasing trend during 1980–2015.

(3) According to the contribution rates of urbanization to precipitation extremes, we conclude that high urbanization tended to have a higher contribution to most extreme precipitation indices, especially the intensity indices, than urbanization in the medium-size cities, indicating that the urbanization leads to the phenomenon of extreme precipitation enhancement.

The extreme precipitation has a complex relationship with many factors, such as the urban heat island effect, canopy barrier effect, and aerosol emissions. So the influence mechanism of urbanization on extreme precipitation remains to be more comprehensive and deeper analysis in future work.

Author Contributions: Conceptualization, C.K. and Z.L.; methodology, C.K.; validation, J.H. and W.Z.; writing—original draft preparation, C.K.; writing—review and editing, J.H.; supervision, Z.L. All authors have read and agreed to the published version of the manuscript.

Funding: This research was funded by the National Natural Science Foundation of China (grant n. 41501570).

Institutional Review Board Statement: Not applicable.

Informed Consent Statement: Not applicable.

Data Availability Statement: The data presented in this study are available on request from the corresponding author.

Acknowledgments: We greatly appreciate the editor and reviewers for their insightful comments and constructive suggestions that helped us to improve the manuscript.

Conflicts of Interest: The authors declare no conflict of interest.

Abbreviations

SXC	Suzhou-Wuxi-Changzhou Urban Agglomeration
WRF	Weather Research and Forecasting Model
GDP	Gross Domestic Product
RMB	Renminbi
CDD	Consecutive Dry Days
CWD	Consecutive Wet Days
SDII	Simple Daily Intensity Index
Rx1day	Maximum One-Day Precipitation
Rx5day	Maximum Five-Day Precipitation
PRCPTOT	Total Wet-Day Precipitation
IAP	The Global Artificial Impervious Area Dataset
POP	Population Dataset
FCM	The Fuzzy C-Means method
MK	Test Mann-Kendall Statistical Test

References

1. Shamshirband, S.; Hashemi, S.; Salimi, H.; Samadianfard, S.; Asadi, E.; Shadkani, S. Predicting standardized streamflow index for hydrological drought using machine learning models. *Eng. Appl. Comput. Fluid Mech.* **2020**, *14*, 339–350. [CrossRef]
2. Dehghani, S.; Salehi, S.; Mosavi, A.; Nabipour, N.; Shamshirband, S.; Ghamisi, P. Spatial analysis of seasonal precipitation over iran: Co-variation with climate indices. *Int. J. Geo-Inf.* **2020**, *9*, 73. [CrossRef]
3. Hallegatte, S.; Green, C.; Nicholls, R.J.; Corfee-Morlot, J. Future flood losses in major coastal cities. *Nat. Clim. Chang.* **2013**, *3*, 802–806. [CrossRef]
4. Huang, L.; Luo, Y.; Zhang, D.L. The relationship between anomalous presummer extreme rainfall over south China and synoptic disturbances. *J. Geophys. Res. Atmos.* **2018**, *123*, 3395–3413. [CrossRef]
5. Pathirana, A.; Denekew, H.B.; Veerbeek, W.; Zevenbergen, C.; Banda, T.A. Impact of urban growth-driven land use change on microclimate and extreme precipitation-a sensitivity study. *Atmos. Res.* **2014**, *138*, 59–72. [CrossRef]
6. Dou, J.; Wang, Y.; Bornstein, R.; Miao, S. Observed spatial characteristics of Beijing urban climate impacts on summer thunderstorms. *J. Appl. Meteor. Clim.* **2015**, *54*, 94–105. [CrossRef]
7. Jun, S.; Linli, C.; Junbang, W.; Huaqiang, D.; Kangmin, W. Changes in the temperature and precipitation extremes in China during 1961–2015. *Quat. Int.* **2018**, *527*, 64–78.
8. Horton, R.E. Thunderstorm-Breeding Spots. *Mon. Weather Rev.* **1921**, *49*, 193. [CrossRef]
9. Changnon, S.A. The La Porte anomaly: Fact or fiction? *B Am. Meteorol. Soc.* **1968**, *49*, 4–11. [CrossRef]
10. Changnon, S.A.; Huff, F.A.; Semonin, R.G. METROMEX: An Investigation of Inadvertent Weather Modification. *B Am. Meteorol. Soc.* **1971**, *52*, 958–968. [CrossRef]
11. Shepherd, J.M.; Burian, S.J. Detection of Urban-Induced Rainfall Anomalies in a Major Coastal City. *Earth Interact.* **2003**, *7*, 1–17. [CrossRef]
12. Ntelekos, A.A.; Smith, J.A.; Donner, L.; Fast, J.D.; Gustafson, W.I.; Chapman, E.G. The effects of aerosols on intense convective precipitation in the northeastern United States. *Q. J. Roy. Meteor. Soc.* **2009**, *135*, 1367–1391. [CrossRef]
13. Trusilova, K.; Jung, M.; Churkina, G. On Climate Impacts of a Potential Expansion of Urban Land in Europe. *J. Appl. Meteorol. Clim.* **2009**, *48*, 1971–1980. [CrossRef]
14. Li, X.X.; Koh, T.Y.; Panda, J.; Norford, L.K. Impact of urbanization patterns on the local climate of a tropical city, Singapore: An ensemble study. *J. Geophys. Res.-Atmos.* **2016**, *121*, 4386–4403. [CrossRef]
15. Wang, J.; Feng, J.; Yan, Z. Potential sensitivity of warm season precipitation to urbanization extents: Modeling study in Beijing-Tianjin-Hebei urban agglomeration in China. *J. Geophys. Res.-Atmos.* **2015**, *120*, 9408–9425. [CrossRef]
16. Zhong, S.; Qian, Y.; Zhao, C.; Leung, R.; Wang, H.; Yang, B.; Fan, J.; Yan, H.; Yang, X.Q.; Liu, D. Urbanization-induced urban heat island and aerosol effects on climate extremes in the Yangtze River Delta region of China. *Atmos. Chem. Phys.* **2017**, *17*, 5439–5457. [CrossRef]

17. Wang, Y.; Chen, L.; Song, Z.; Zeqing, H.; Erjia, G.; Lijie, L. Human-perceived temperature changes over South China: Long-term trends and urbanization effects. *Atmos. Res.* **2019**, *215*, 116–127. [CrossRef]
18. Wu, M.; Luo, Y.; Chen, F.; Wong, W.K. Observed Link of Extreme Hourly Precipitation Changes to Urbanization over Coastal South China. *J. Appl. Meteorol. Clim.* **2019**, *58*, 1799–1819. [CrossRef]
19. Paul, S.; Ghosh, S.; Mathew, M.; Devanand, A.; Karmakar, S.; Niyogi, D. Increased Spatial Variability and Intensification of Extreme Monsoon Rainfall due to Urbanization. *Sci. Rep.* **2018**, *8*, 3918. [CrossRef]
20. Huang, Y.; Liu, Y.; Liu, Y.; Li, H.; Knievel, J.C. Mechanisms for a record-breaking rainfall in the coastal metropolitan city of Guangzhou, China: Observation analysis and nested very large eddy simulation with the WRF Model. *J. Geophys. Res.* **2019**, *124*, 1370–1391. [CrossRef]
21. Yang, L.; Smith, J.; Niyogi, D. Urban Impacts on Extreme Monsoon Rainfall and Flooding in Complex Terrain. *Geophys. Res. Lett.* **2019**, *46*, 5918–5927. [CrossRef]
22. Hopmans, J.W.; Pasternack, G. Experimental hydrology: A bright future. *Adv. Water Resour.* **2006**, *29*, 117–120. [CrossRef]
23. Lu, M.; Xu, Y.; Shan, N.; Wang, Q.; Yuan, J.; Wang, J. Effect of urbanisation on extreme precipitation based on nonstationary models in the Yangtze River Delta metropolitan region. *Sci. Total Environ.* **2019**, *673*, 64–73. [CrossRef] [PubMed]
24. Ragno, E.; Aghakouchak, A.; Cheng, L.; Sadegh, M. A generalized framework for process-informed nonstationary extreme value analysis. *Adv. Water Resour.* **2019**, *130*, 270–282. [CrossRef]
25. Wang, J.; Feng, J.M.; Yan, Z.W. Impact of extensive urbanization on summertime rainfall in the Beijing region and the role of local precipitation recycling. *J. Geophys. Res.-Atmos* **2018**, *123*, 3323–3340. [CrossRef]
26. Zhuang, Q.; Liu, S.; Zhou, Z. Spatial Heterogeneity Analysis of Short-Duration Extreme Rainfall Events in Megacities in China. *Water* **2020**, *12*, 3364. [CrossRef]
27. Ren, M.; Xu, Z.; Pang, B.; Liu, J.; Du, L. Spatiotemporal Variability of Precipitation in Beijing, China during the Wet Seasons. *Water* **2020**, *12*, 716. [CrossRef]
28. Ma, B.; Wu, Z.; Wang, H.; Guo, Y. Study on the Classification of Urban Waterlogging Rainstorms and Rainfall Thresholds in Cities Lacking Actual Data. *Water* **2020**, *12*, 3328. [CrossRef]
29. Zhou, Q. A Review of Sustainable Urban Drainage Systems Considering the Climate Change and Urbanization Impacts. *Water* **2014**, *6*, 976–992. [CrossRef]
30. Ye, C.H.; Sun, C.W.; Chen, L.T. New evidence for the impact of financial agglomeration on urbanization from a spatial econometrics analysis. *J. Clean Prod.* **2018**, *200*, 65–73. [CrossRef]
31. Jia, N.; Sitzenfrei, R.; Rauch, W.; Liang, S.; Liu, Y. Effects of Urban Forms on Separate Drainage Systems: A Virtual City Perspective. *Water* **2019**, *11*, 758. [CrossRef]
32. Guo, J.; Pan, Y.; Zuo, P.; Xu, Y.; Wang, Q.; Ma, J.; Wang, L. Accumulation and wash-off characteristics of surface pollutant and identification of risk areas on urban land uses in a lakeside city, Wuxi, China. *Urban Water J.* **2019**, *16*, 323–333. [CrossRef]
33. Geng, Y.; Zhu, B.; Zheng, X. Effect of Independent Variables on Urban Flood Models. *Water* **2020**, *12*, 3442. [CrossRef]
34. Shawul, A.A.; Chakma, S. Trend of extreme precipitation indices and analysis of long-term climate variability in the Upper Awash basin, Ethiopia. *Theor. Appl. Climatol.* **2020**, *140*, 635–652. [CrossRef]
35. Gong, P.; Li, X.; Wang, J.; Bai, Y.; Zhou, Y. Annual maps of global artificial impervious area (GAIA) between 1985 and 2018. 2020. *Remote Sens. Environ.* **2020**, *236*, 111510. [CrossRef]
36. Kulkarni, A.; Kripalani, R.H. Rainfall Patterns over India: Classification with Fuzzy c-Means Method. *Theor. Appl. Climatol.* **1998**, *59*, 137–146. [CrossRef]
37. Mohd-Safar, N.Z.; Ndzi, D.; Sanders, D.; Noor, H.M.; Kamarudin, L.M. Integration of fuzzy c-means and artificial neural network for short-term localized rainfall forecasting in tropical climate. In *Proceedings of SAI Intelligent Systems Conference*; Springer: Cham, Amsterdam, 2016; pp. 325–348.
38. Rodgers, K.; Roland, V.; Hoos, A.; Crowley-Ornelas, E.; Knight, R. An Analysis of Streamflow Trends in the Southern and Southeastern US from 1950–2015. *Water* **2020**, *12*, 3345. [CrossRef]
39. Worku, G.; Teferi, E.; Bantider, A.; Dile, Y.T. Observed changes in extremes of daily rainfall and temperature in Jemma Sub-Basin, Upper Blue Nile Basin, Ethiopia. *Theor. Appl. Climatol.* **2019**, *135*, 839–854. [CrossRef]
40. Zhao, N.; Jiao, Y.; Ma, T.; Zhao, M.; Yue, T. Estimating the effect of urbanization on extreme climate events in the Beijing-Tianjin-Hebei region, China. *Sci. Total Environ.* **2019**, *688*, 1005–1015. [CrossRef]